analytical chemistry
Article
pubs.acs.org/ac

Improving Secondary Ion Mass Spectrometry C_{60}^{n+} Sputter Depth Profiling of Challenging Polymers with Nitric Oxide Gas Dosing

R. Havelund,*,† A. Licciardello,‡ J. Bailey,§ N. Tuccitto,‡ D. Sapuppo,‡ I. S. Gilmore,† J. S. Sharp,§ J. L. S. Lee,† T. Mouhib,∥,⊥ and A. Delcorte∥

†National Physical Laboratory, Teddington, Middlesex, TW11 0LW, United Kingdom

‡Laboratory for Molecular Surfaces and Nanotechnology (LAMSUN), Dipartimento di Scienze Chimiche, Università degli Studi di Catania and CSGI, Via A. Doria 6, 95125 Catania, Italy

§School of Physics and Astronomy and Nottingham Nanotechnology and Nanoscience Centre, University of Nottingham, University Park, Nottingham, NG7 2RD, United Kingdom

∥Institute of Condensed Matter and Nanosciences-Bio & Soft Matter, Université Catholique de Louvain, Croix du Sud, 1 bte L7.04.01; B-1348 Louvain-la-Neuve, Belgium

S Supporting Information

ABSTRACT: Organic depth profiling using secondary ion mass spectrometry (SIMS) provides valuable information about the three-dimensional distribution of organic molecules. However, for a range of materials, commonly used cluster ion beams such as C_{60}^{n+} do not yield useful depth profiles. A promising solution to this problem is offered by the use of nitric oxide (NO) gas dosing during sputtering to reduce molecular cross-linking. In this study a C_{60}^{2+} ion beam is used to depth profile a polystyrene film. By systematically varying NO pressure and sample temperature, we evaluate their combined effect on organic depth profiling. Profiles are also acquired from a multilayered polystyrene and polyvinylpyrrolidone film and from a polystyrene/polymethylmethacrylate bilayer, in the former case by using an optimized set of conditions for C_{60}^{2+} and, for comparison, an Ar_{2000}^{+} ion beam. Our results show a dramatic improvement for depth profiling with C_{60}^{2+} using NO at pressures above 10^{-6} mbar and sample temperatures below −75 °C. For the multilayered polymer film, the depth profile acquired using C_{60}^{2+} exhibits high signal stability with the exception of an initial signal loss transient and thus allows for successful chemical identification of each of the six layers. The results demonstrate that NO dosing can significantly improve SIMS depth profiling analysis for certain organic materials that are difficult to analyze with C_{60}^{n+} sputtering using conventional approaches/conditions. While the analytical capability is not as good as large gas cluster ion beams, NO dosing comprises a useful low-cost alternative for instruments equipped with C_{60}^{n+} sputtering.

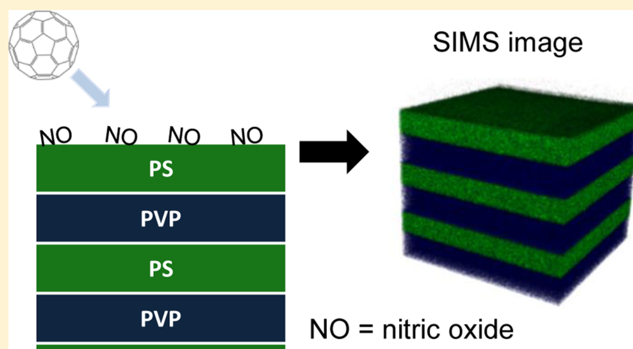

Knowledge of the three-dimensional distribution of organic molecules is important to the innovation and manufacture of many advanced technologies including polymer electronics and photovoltaics,[1] polymer optical filters and reflectors,[2,3] inkjet printing technologies,[4] and drug delivery systems.[5,6] Organic depth profiling using sputtering with cluster ion beams and imaging by SIMS has revolutionized the analytical capability for these systems, providing detailed 3D chemical information.[7] However, the cluster ion beams of choice during recent years (C_{60}^{n+} and SF_5^{+}) work only for a limited set of materials and fail for other materials due to damage build-up and roughening caused by the sputter ion beam.[8,9] A particularly challenging set of molecules are polymers that cross-link under ion irradiation. These include industrially important polymers such as polyethylene, polystyrene, and conjugated polymers, such as those used in the organic electronics industry. Sample cooling,[8,10,11] sample rotation,[11] and grazing ion beam incidence angle[12,13] have been reported to improve the analytical capability of SF_5^{+} and C_{60}^{n+} sputter depth profiling, yet, attempts to depth profile the "problem materials" generally result in poor profiles containing very little useful chemical or depth distribution information.

Recently, argon gas cluster ion beams have become available and allow for depth profiling with minimal chemical degradation,[14] constant sputtering yields,[15] and the best depth resolution currently achievable.[16] However, C_{60}^{n+} and SF_5^{+} ion beams are currently more widespread than argon gas cluster ion beams and will continue to be widely used. Consequently, an important development is the use of nitric oxide (NO) dosing as a radical scavenger to reduce ion

Received: February 1, 2013
Accepted: April 16, 2013
Published: April 16, 2013

 © 2013 American Chemical Society

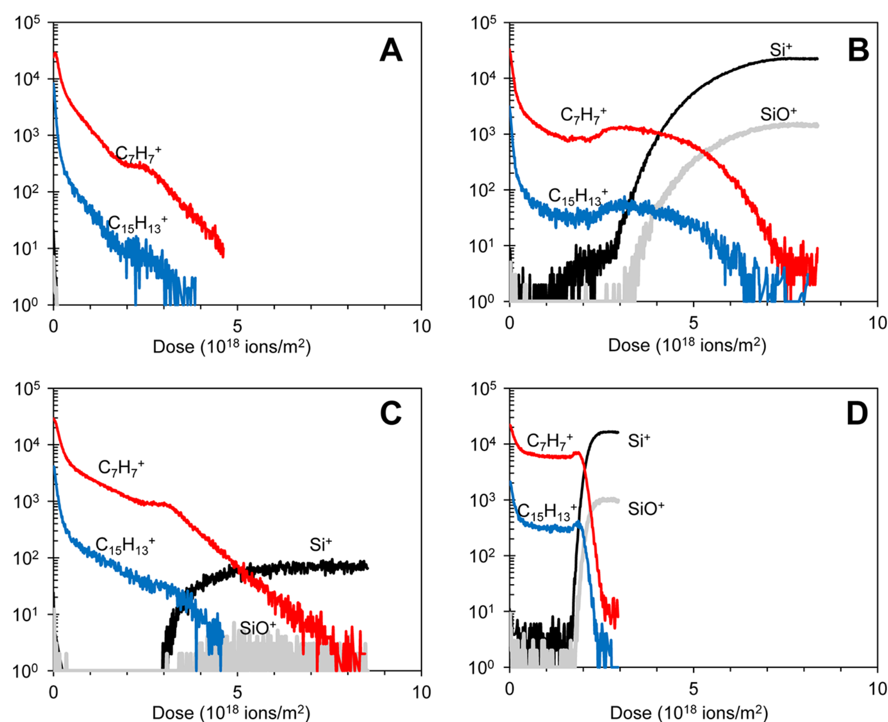

Figure 1. SIMS depth profiles from 77 nm PS on a silicon substrate acquired at four different conditions. (A) 25 °C without NO dosing ("standard conditions"), (B) 25 °C and 1×10^{-5} mbar NO, (C) −100 °C without NO dosing, (D) −100 °C, 1×10^{-5} mbar NO. Shown secondary ion signals are Si^+ (black) and SiO^+ (gray) for the substrate and $C_7H_7^+$ (red) and $C_{15}H_{13}^+$ (blue) for PS.

bombardment induced cross-linking during depth profiling. The approach was introduced by Tuccitto et al. at the 17th International Conference on Secondary Ion Mass Spectrometry[17] who showed that when a film of polystyrene was flooded with NO gas, a stable secondary ion yield could be maintained to sampling depths above 900 nm. Briefly, under ion beam irradiation of organic materials, bonds break and radicals can be formed. These may react to cross-link the material. When this happens, the sputtering yield drops significantly so that there is an imbalance in the volume of damaged material created by the ion beam and the volume of material sputtered away to expose fresh material.

Nitric oxide is an odd-electron molecule with the highest-energy occupied molecular orbital containing one electron mostly localized on nitrogen. Consequently, it is a radical and will react with other radicals to suppress or reduce cross-link formation in the material. In this study, we use a C_{60}^{2+} ion beam to sputter depth profile a polystyrene layer in order to evaluate the basic metrology and give recommendations for the use of NO dosing in combination with sample cooling. Further details about the chemical mechanism will be given in a separate publication. Here, we provide analysts with a measure of the effectiveness of NO dosing. We demonstrate the benefits of NO dosing on a multilayered polystyrene and polyvinylpyrrolidone model system and compare the depth profiling performance with a state-of-the-art argon gas cluster ion beam.

EXPERIMENTAL SECTION

A thin film of polystyrene (PS) on silicon was prepared by spincoating PS (MW_{av} = 2500) from a toluene solution onto a 10 mm × 10 mm silicon wafer piece at 3000 rpm for 180 s. The film thickness was mapped across the sample with an M-2000 spectroscopic ellipsometer (Woollam) and was found to be uniform with a thickness value of 77 ± 1 nm over a 5 mm × 5 mm area.

A six-layer polymer structure was manufactured by sequentially spincoating polymers from mutual exclusive (orthogonal) solvents onto a silicon substrate.[2] Polymer solutions of PS (MW_{av} = 192 000, Sigma, U.K.) and polyvinylpyrrolidone (PVP) (MW_{av} = 1 300 000, BASF, Germany) were prepared in toluene and ethanol/acetonitrile (50/50 weight ratio), respectively. The PVP solution was used to produce layers with thickness values of 247.9 ± 2.6 nm at 2710 rpm whereas the PS films had thickness values of 194.5 ± 3.0 nm at 3040 rpm. The thickness values were determined through a series of parallel measurements. A home-built self-nulling ellipsometer (wavelength λ = 633 nm) was used to measure single polymer films that were produced using the same deposition parameters used to manufacture the multilayers. The polymer layer thickness values in this system were found to be independent of the substrate on which the layers were deposited (silicon or polymer). It was found that the production of high-quality multilayers required the PVP layers to be protected by swelling with HCl vapor. This swelling step prevents the diffusion of toluene through the PVP layer and swelling of underlying PS layers. FT-IR analysis showed that no chemical changes occurred in the PVP or PS when swelling the polymer multilayer with HCl.[3] The samples were annealed for 5 h at 110 °C under vacuum (~10^{-3} mbar) to remove residual solvent and HCl vapor and also to relieve spincoating stresses.

Finally, a bilayer consisting of PS (Scientific Polymer Products, MW_{av} = 280 000) supported on polymethylmethacrylate (PMMA, Scientific Polymer Products, MW_{av} = 540 000) was prepared on a cleaned silicon wafer substrate by spincoating at 1500 rpm for 60−90 s from 3% solutions in 1-chloropentane and chloroform solutions, respectively, in

order to obtain approximately 0.5 μm thick layers (thickness value estimated from previous measurements).

SIMS depth profiles of the PS/Si and PS/PVP samples were acquired using a TOF−SIMS IV (ION−TOF GmbH, Münster, Germany) at the National Physical Laboratory (NPL). The instrument is equipped with a C_{60}^{n+} ion beam for sputtering and a liquid metal ion beam with a combined Bi and Mn emitter[18] for analysis. A pulsed 20 keV C_{60}^{2+} ion beam was raster scanned for sputtering of the samples over an area of 500 μm × 500 μm. In between sputtering pulses, a Bi_3^+ ion pulse (25 keV, 0.2 pA) was used for SIMS analysis in the central 300 μm × 300 μm of the sputter crater. For comparison, the PS/PVP sample was further depth profiled using a 5 keV Ar_{2000} ion beam for sputtering. The relative dose of the analysis and sputtering beams was 0.2% so sputtering and damage caused by the analysis beam can be disregarded.[19,20] To reduce charging of the PS/PVP samples, the samples were flooded with 20 eV electrons with an on-target current of approximately 10 μA. The PS/PMMA bilayer sample was analyzed with a similar instrument at the University of Catania. The 20 keV C_{60}^{2+} ion beam was set to sputter a 200 μm × 200 μm area, with the bismuth analysis beam analyzing a concentric 130 μm × 130 μm region.

In this study, nitric oxide (NO) gas (98.5%, Sigma-Aldrich at NPL and Rivoira-Praxair at University of Catania) was used. NO is highly toxic and reacts instantly with water and oxygen to form nitrous acid. It is imperative that special precautions are used and a full risk assessment is conducted. The gas handling system used in the NPL instrument was constructed and tested by experts in gas metrology at NPL. Similarly, the system at the University of Catania was constructed and tested by in-house experts. NO is delivered to the sample through a needle-valve into the vacuum system via a narrow pipe with an outlet approximately 10 mm from the sample surface. The NO gas was maintained in the range from 10^{-8} to 10^{-5} mbar and was measured as the total pressure in the vacuum chamber (the vacuum base pressure was around 10^{-9} mbar). It should be noted that this is not a measurement of the NO pressure above the sample since the ion gauge is located beneath the sample and closer to the turbomolecular vacuum pump. This measurement is therefore system-specific and the amount of gas depends on the instrument setup, e.g., the type and location of the gas inlet and the location of the pressure gauge. The sample temperature was controlled between −125 and 50 °C by balancing indirect liquid nitrogen cooling of the sample with a heating wire using a sample heating/cooling stage provided by the instrument manufacturer.

RESULTS AND DISCUSSION

Figure 1 shows the positive ion depth profiles of PS/Si acquired with and without NO dosing at −100 and 25 °C. The PS layer is represented by $C_7H_7^+$ and $C_{15}H_{13}^+$, the substrate by Si^+ and SiO^+. Alternative figures showing other secondary ion profiles can be found in the Supporting Information, Figures S-1−S-4. At room temperature without NO (A), the signal intensity rapidly degrades and no ions from the substrate are seen in this experiment. At −100 °C without NO (B), PS signal intensity is observed, albeit strongly declining, up to the interface. Only weak substrate signals are observed, presumably owing to the build-up of a cross-linked carbonaceous overlayer on the sample indicated by a continuous increase in C^+ signal (see Figure S-1 in the Supporting Information). A similar result is obtained when using NO at room temperature (C). While NO dosing and sample cooling do have an effect when applied individually, it is the result of the combination of the two that gives the best performance. The depth profile acquired at −100 °C with NO at a pressure of 1×10^{-5} mbar (D) exhibits a sharp well-defined signal change at the PS/Si interface as well as a high, nearly stable signal for relevant characteristic ions in the (steady−state) region between the surface and the PS/Si interface and into the silicon substrate. The C_{60}^{2+} dose required to reach the interface is lower at −100 °C with NO dosing, indicating that the formation of a cross-linked overlayer is reduced compared to the other conditions.

To study the combined effect of cooling and NO dosing in detail, a series of depth profiles were made by (1) varying the sample temperature while keeping the NO pressure at 1×10^{-5} mbar and (2) varying the NO pressure while keeping the sample at −100 °C. The SIMS depth profiles can be analyzed based on the erosion dynamics model.[21] Shard et al.[22,23] showed that a steady state is not achieved if the sputtering rate is not constant owing to a build-up of damage or increasing surface topography. Wucher[24] has also included the effect of a dose dependent sputtering rate in the erosion dynamics model. Here, we use this model to characterize the effects of changing the NO pressure and the sample temperature on the depth profile. The model applies to molecular ions and not fragment ions which are used to identify a polymer. Still, the model is found to provide a good description of the $C_7H_7^+$ depth profiles. As an example, the erosion dynamics model fit to the depth profile acquired at −100 °C with NO at a pressure of 1×10^{-5} mbar is shown in Figure 2.

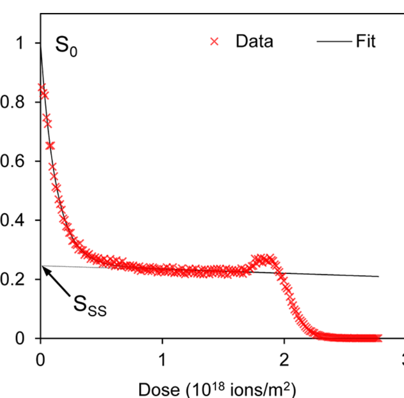

Figure 2. Erosion dynamics model fit to $C_7H_7^+$ signal at −100 °C and 1×10^{-5} mbar NO. Fitting parameters are $a = 0.04$ nm²/ion and $\varepsilon = 0.37$ corresponding to $S_{SS}/S_0 = 0.27$.

Two parameters are used for fitting the model to the secondary ion signal. The yield decay cross section, a, relates the total sputtering yield, Y_{tot}, to the sputtering ion dose, d, by eq 1.

$$Y_{tot}(d) = Y_{tot}(0)[1 - a \cdot d] \quad (1)$$

The change in sputtering yield is typically not linear,[22,23] but this is found to be a reasonable approximation here. In a depth profile, $a > 0$ is reflected in a continuously degrading signal (the signal is proportional to the product of the surface concentration of the molecule, or fragment, and the total sputtering yield).

The cleanup efficiency, ε, is the fraction of the damage created by an ion impact that is removed by the same impact. In a depth profile, ε is expressed in the exponential signal loss

observed in the beginning of the profile. Equation 2 relates ε to the secondary ion signal in the steady state (S_{SS}) relative to the initial signal (S_0).

$$\frac{S_{SS}}{S_0} = \frac{\varepsilon}{1 + \varepsilon} \quad (2)$$

If a true steady state is not achieved, $a \neq 0$, the steady state intensity in eq 2 is determined by extrapolating the signal in the linear yield decay region back to $d = 0$, as shown in Figure 2. For the formal description of how the secondary ion signal relates to the two parameters, the reader is referred to Wucher.[24]

Figure 3A shows the cleanup efficiency and yield decay cross section as a function of sample temperature. By cooling the sample from 50 to −125 °C while keeping the NO pressure at 1×10^{-5} mbar, the cleanup efficiency improves by a factor of 5. Furthermore, the sputtering yield was almost constant at the lowest temperature. In addition to the known benefit of depth profiling at low sample temperature,[8,10,11] the observed improvement is believed to be a consequence of the resulting increase in the amount of physisorbed NO on the sample surface and decrease in the rate-constant for radicals to cause cross-linking. The instrument at the University of Catania exhibited similar values for the cleanup efficiency with $\varepsilon = 0.13$ at 25 °C and 1×10^{-5} mbar compared with $\varepsilon = 0.08$ in Figure 3 for the NPL instrument. This difference is likely to be due to the pressure not being measured directly above the sample surface and may depend on pumping speeds and other instrumental configuration effects, for example, the University of Catania instrument has a larger main chamber than the NPL instrument.

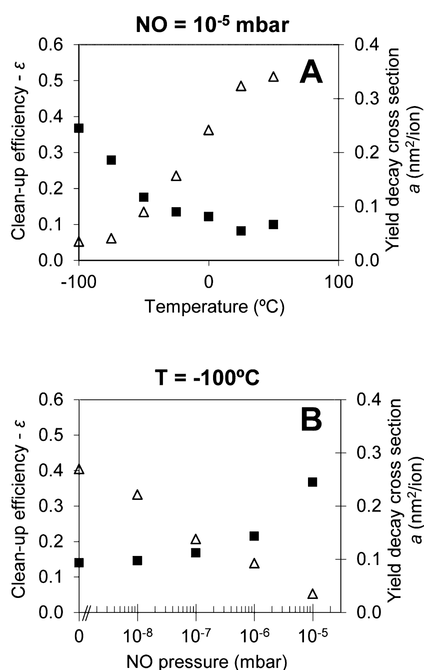

Figure 3. Clean-up efficiency (■) and yield decay cross section (Δ) for 20 keV C_{60}^{2+} on PS determined for $C_7H_7^+$ signal as a function of (A) sample temperature (NO pressure 1×10^{-5} mbar) and (B) NO pressure (sample temperature −100 °C).

Similarly, Figure 3B shows that increasing the NO pressure from 1×10^{-8} mbar to 1×10^{-5} mbar while keeping the temperature at −100 °C improves both parameters; in particular between 1×10^{-6} mbar and 1×10^{-5} mbar. Further improvements are, in principle, likely to be evident by cooling the sample to an even lower temperature or increasing the amount of NO available; however, the latter is critically constrained by the pressure sensitivity of the SIMS instrument. On the basis of these measurements, we recommend that if using NO, a pressure of 1×10^{-5} mbar (setup specific, see Experimental Section) is selected along with the lowest achievable stable sample temperature below −75 °C.

It was observed that good depth profiles of samples that required charge neutralization by electron flooding could not be consistently achieved with these recommended parameters. In some cases, the depth profiles showed clear signs of sample charging (Supporting Information, Figure S-5). It was thus realized that NO, as well as scavenging radical electrons, also scatters or reacts with electrons from the low energy electron flood gun. This reduces the electron current to the sample and the effectiveness of charge neutralization. This hypothesis was confirmed by measuring the electron current at the sample as a function of NO pressure. Increasing the NO pressure to 8.5×10^{-6} mbar reduced the effective electron current from 1.3 μA to 0.3 μA (see the Supporting Information, Figure S-6), which, for depth profiling experiments where the sputtering ion dose is higher than in static SIMS, is often insufficient for successful charge neutralization. To limit the impact of this effect, the ion beam current densities need to be reduced so that only a low electron current density is required. Note that the corollary to this is that increasing the low energy electron current may reduce the amount of NO available to scavenge radicals and consequently degrade the profile quality. This is an unfortunate combination since most industrially relevant samples are insulating.

The ability to obtain depth profiles beyond a simple homogeneous polymer film with C_{60}^{2+} sputtering and NO dosing was evaluated by depth profiling a multilayered PS/PVP film at −100 °C and 1×10^{-5} mbar NO pressure. Figure 4A shows the positive ion depth profile. Each of the six layers in the film are chemically identifiable with $C_7H_7^+$ characteristic of PS and $C_4H_5O^+$ characteristic of PVP. The profile exhibits clear separation of the adjacent layers by a well-defined interface. For

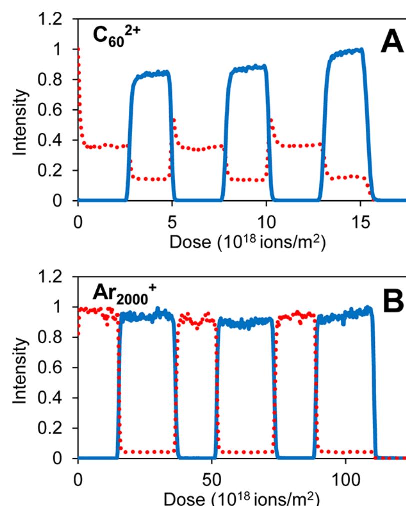

Figure 4. Positive ion depth profiles from PS/PVP multilayer samples with (A) C_{60}^{2+} sputtering and (B) Ar_{2000}^+ sputtering, showing the $C_7H_7^+$ signal in red (dashed) for PS and $C_4H_5O^+$ signal in blue (solid) for PVP. Each signal is normalized to its maximum value.

Table 1. Average Sputtering Yield Volume for Each of the Six Layers from Top to Bottom (1−6)

layer	1 PS	2 PVP	3 PS	4 PVP	5 PS	6 PVP
layer thickness (nm)	194.5 ± 3.0	248 ± 2.6	195 ± 3.0	248 ± 2.6	195 ± 3.0	248 ± 2.6
SYV(C_{60}^{2+} + NO) (nm^3)	70.1 ± 1.1	113.3 ± 1.9	67.1 ± 1.0	109.4 ± 1.9	65.7 ± 1.0	108.3 ± 1.8
SYV($Ar2000^+$) (nm^3)	12.7 ± 0.3	11.7 ± 0.2	12.6 ± 0.3	11.6 ± 0.2	12.5 ± 0.3	11.4 ± 0.2

Table 2. Depth Resolution Parameters in the Top Five Polymer Layers from Top to Bottom (1−5)[a]

layer	1 PS	2 PVP	3 PS	4 PVP	5 PS
layer thickness (nm)	194.5 ± 3.0	248 ± 2.6	195 ± 3.0	248 ± 2.6	195 ± 3.0
16%−84% (C_{60}^{2+} + NO) (nm)	13.3 ± 2.1	17.7 ± 3.4	14.0 ± 2.0	20.5 ± 3.3	16.2 ± 2.0
fwhm (C_{60}^{2+} + NO) (nm)	15.7 ± 2.5	20.8 ± 4.0	16.5 ± 2.4	24.1 ± 3.9	19.1 ± 2.4
16%−84% (Ar_{2000}^+) (nm)	6.8 ± 0.4	10.7 ± 0.7	7.3 ± 0.5	11.0 ± 0.7	7.6 ± 0.5
fwhm (Ar_{2000}^+) (nm)	8.0 ± 0.5	12.6 ± 0.8	8.6 ± 0.6	13.0 ± 0.8	8.9 ± 0.6

[a]The depth resolution parameter is measured from the 16% to 84% intensity change across an interface corresponding to 2σ of a Gaussian response function (see text). The fwhm is derived as $(2\ln(2))^{1/2}2\sigma$ and is provided for comparison with previously published work.

comparison, the positive ion depth profile from the same sample obtained using an Ar_{2000}^+ ion beam is shown in Figure 4B. From these data, the depth profiling with C_{60}^{2+} was overall successful, though clearly not as good as with argon clusters. For example, attention should be given to certain features in the C_{60}^{2+}depth profile. First, an exponential decay of the $C_7H_7^+$ signal was not only observed at the top surface but also in the initial parts of the two deeper PS layers. This behavior indicates that damage was built-up when entering the PS layers until a steady state was reached and was "cleaned up" when entering the PVP layers. The damage formation following the PVP/PS interface is further likely to cause the sputtering rate to drop rapidly in these regions in which case a depth scale within the PS layers cannot be accurately established from the ion dose. The profile obtained with the argon cluster ion beam does not have similar transient effects which reflects the minimal damage induced by large clusters with low energy per cluster ion atom and indicates a constant sputtering yield within each layer. Recent molecular dynamics simulations have estimated the amount of cross-linking for C_{60}^{n+} and argon cluster projectiles.[25] The simulations show that the amount of cross-linking is higher for C_{60}^{n+} because the additional carbon radicals originating from the projectile contribute to the creation of new intermolecular bonds. This study also indicates that cross-linking will reduce for larger clusters.

The $C_7H_7^+$ signal in the C_{60}^{2+} profile does not show as high a contrast between the PS and PVP layers as in the Ar_{2000}^+ profile, presumably because of the increased fragmentation with C_{60}^{2+} sputtering which leads to the formation of $C_7H_7^+$ as a damage product from PVP. In addition, damage build-up generally decreases the characteristic ion signals in the PS layers. Reactions between the polymers and the oxidizing NO also cause differences in relative signal intensities, however, for PS and PVP the mass spectra obtained with NO largely resemble spectra obtained from the same materials without NO (data not shown) so such chemical effects do not critically affect the overall chemical identification.

The position of the polymer/polymer interfaces is here defined as the dose at which 50% of the total signal intensity change across the interface has taken place. The width of the interface can be calculated as the dose difference between the 16% level and the 84% level on the intensity scale (equivalent to 2σ of a Gaussian function convoluted with a step edge). These measures allow for calculating average sputtering yield volume and estimating a depth resolution parameter, 16%−84%, in each layer.

For C_{60}^{2+}, the average sputtering yield volume (Table 1) is significantly lower in the PS layers than in the PVP layers. This observation is consistent with damage building up in the PS layers which causes the sputtering to slow down. Consequently, the sputtering rate change across the PS-to-PVP interfaces (top-to-bottom) is larger than the numbers in Table 1 indicate. Furthermore, Table 1 shows that the average sputtering yield volume decays with increasing sampling depth, as has previously been observed.[22] For Ar_{2000}^+, the sputtering yield volumes for PVP and PS are similar and the sputtering yield volume is constant with increasing sampling depth. The sputtering yield volumes for PVP are comparable with those reported earlier by Mouhib et al. of 93 nm^3 with 15 keV C_{60}^+ sputtering.[26]

Because of the large and unknown change in sputtering rate across the interfaces for C_{60}^{2+}, the measured interface widths do not allow for determining depth resolution accurately. In fact, the change in sputtering rate across the interfaces conflicts with the commonly used definitions of depth resolution which require linearity between dose and depth. For this reason, it is only possible to calculate a depth resolution parameter which is an estimate of the real depth resolution based on choices made for the calculation. Here, we take the interface width for the falling signal at the interface below a layer and use the sputtering rate for this layer as a conversion factor to estimate the depth resolution parameter, 16%−84%, in the first five layers from the top as given in Table 2. The estimate will give the actual depth resolution if (1) the SIMS response function is Gaussian, (2) the sputtering yield volume in the region near the interface does not depend on the sputtering yield volume of the polymer below the interface, and (3) the interface is sharp. If all three criteria are met, the interface width measured for the falling (and rising) signal at an interface will only depend on the sputtering rate in the layer above the interface and the width will be 2σ of the Gaussian response function. This is generally not the case, yet, the depth resolution parameter used here is sufficient to allow for comparison between different experimental conditions. We also provide in Table 2 the depth resolution as the corresponding fwhm of a Gaussian $(2\ln(2))^{1/2}2\sigma$ calculated from the 16%−84% value for

convenient comparison with previous studies where that parameter is measured directly.

The measured depth resolution parameter range as well as the tendency to degrade with increasing sampling depth is in agreement with previous studies on depth profiling using $C_{60}{}^{n+}$ ion beams. Previously, Mouhib et al.[26] in their study of a PVP/PMMA bilayer showed that useful profiles are obtained from PVP with 15 keV $C_{60}{}^{+}$ sputtering and a good interface with the PMMA layer is observed with a width of 16 nm using the 16% to 84% definition. This is comparable to the values reported here. However, it is exceptional that a useful depth resolution is maintained to sampling depths of several hundred nanometers. This clearly demonstrates that the use of NO dosing significantly extends the analytical capability of $C_{60}{}^{n+}$ sputtering of, otherwise, challenging polymers. It is also clear that sputtering using argon clusters is superior and is recommended if available. The excellent depth resolution for $Ar_{2000}{}^{+}$ is likely to be the result of the lower sputtering yield. Previous studies have shown a linear correlation between the cube root of the sputtering yield and the depth resolution[16,27] which is supported by the data presented here.

Finally, in order to confirm the applicability of NO dosing to samples where polymers with different behavior under $C_{60}{}^{n+}$ sputtering coexist, we profiled a PS/PMMA sample. This was conducted at room temperature and demonstrates the performance that may be expected for instruments without special sample cooling capabilities. Good depth profiles of PMMA are achieved with $C_{60}{}^{n+}$ sputtering without the need for NO dosing.[10] However, with an overlayer of PS, damage rapidly builds up so that the PMMA layer is either not reached or characteristic ions are not present in the mass spectrum. In Figure 5, we show the depth profile using the instrument at the University of Catania with NO dosing at the recommended pressure of 1×10^{-5} mbar. This shows that the two different polymer layers are clearly distinguished. The time required for each layer to sputter away (both of comparable thickness) is similar, indicating similar sputtering yields. The profile shows that the characteristic ions for PS increase in intensity in the PMMA layer. This is an important artifact that needs to be considered and is caused by two effects. (1) A cleanup efficiency of 0.13 results in the intensities to fall to a plateau of around 10% of the initial intensities in the PS layer and (2) $C_{60}{}^{2+}$ sputtering causes significant fragmentation in the PMMA material resulting in the formation of the same ions from damage products. These effects may be mitigated by either sample cooling or preferably, if available, using argon cluster sputtering instead as demonstrated in Figure 4.

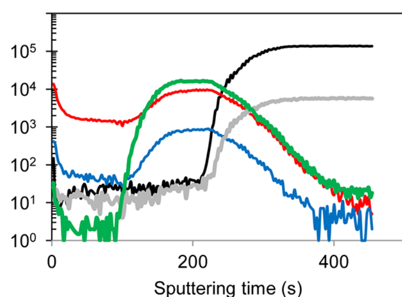

Figure 5. Positive ion depth profile from a PS/PMMA bilayer with an approximate thickness of 1 μm on a silicon wafer substrate obtained at room temperature using $C_{60}{}^{2+}$ sputtering with NO dosing at 1.5×10^{-5} mbar pressure. Shown secondary ion signals are $^{28}Si^{+}$ (black) and $^{30}Si^{+}$ (gray) for the substrate, $C_7H_7{}^{+}$ (red) and $C_{15}H_{13}{}^{+}$ (blue) for PS and $C_4H_5O^{+}$ (green) for PMMA.

CONCLUSION

This study demonstrates that depth profiling of organic molecules and polymers that cross-link under $C_{60}{}^{n+}$ bombardment can be significantly improved by dosing the sample surface with NO. Further improvements can be obtained by employing sample cooling. Using a NO background pressure at 1×10^{-5} mbar and sample temperatures below −75 °C, depth profiles are characterized by low initial characteristic signal loss as well as low dose dependency of signal, sputtering rate, and depth resolution even at sampling depths above 1000 nm. The depth resolution does degrade with increasing sampling depth but is in the range that is typically observed when $C_{60}{}^{n+}$ ion beams are applied to samples that sputter under normal conditions.

Sputtering with argon cluster ions is shown to have superior performance. However, for analysts using $C_{60}{}^{n+}$ ion beams, NO dosing extends the range of materials that can be analyzed without the additional cost of another ion beam. As the mechanism of action is largely independent of the ion beam itself, NO dosing also has the potential to be used alongside other ion beams and in addition to other developments that improve depth profiling, such as sample rotation.

We emphasize that appropriate safety precautions must be taken whenever handling NO due to its highly poisonous nature. We do not recommend installation of a dosing system or any use of NO without seeking expert advice and instruction.

ASSOCIATED CONTENT

Supporting Information

Additional information as noted in text. This material is available free of charge via the Internet at http://pubs.acs.org.

AUTHOR INFORMATION

Corresponding Author

*E-mail: rasmus.havelund@npl.co.uk.

Present Address

⊥T.M.: High School of Technology, Université Hassan 1er, Passage d'Alger, B.P.: 218, 26100 Berrechid, Morocco.

Notes

The authors declare no competing financial interest.

ACKNOWLEDGMENTS

The authors would like to thank Dr. Alexander G. Shard and Dr. Martin P. Seah for helpful comments and Ian Uprichard and Gergely Vargha for expert advice on commissioning the NO dosing system at NPL. This work forms part of the Chemical and Biological Programme of the National Measurement System of the UK Department of Business, Innovation and Skills. T. Mouhib further acknowledges the European Commission for financial support through an ERASMUS Staff Mobility grant.

REFERENCES

(1) Van Duren, J. K. J.; Yang, X. N.; Loos, J.; Bulle-Lieuwma, C. W. T.; Sieval, A. B.; Hummelen, J. C.; Janssen, R. a. J. *Adv. Funct. Mater.* **2004**, *14*, 425−434.

(2) Bailey, J.; Sharp, J. S. *Eur. Phys. J. E* **2010**, *33*, 41−49.

(3) Bailey, J.; Sharp, J. S. *J. Polym. Sci., Part B: Polym. Phys.* **2011**, *49*, 732−739.

(4) Sodhi, R. N. S.; Sun, L.; Sain, M.; Farnood, R. *J. Adhes.* **2008**, *84*, 277−292.
(5) Belu, A. M.; Davies, M. C.; Newton, J. M.; Patel, N. *Anal. Chem.* **2000**, *72*, 5625−5638.
(6) Fisher, G. L.; Belu, A. M.; Mahoney, C. M.; Wormuth, K.; Sanada, N. *Anal. Chem.* **2009**, *81*, 9930−9940.
(7) Mahoney, C. M. *Mass Spectrom. Rev.* **2010**, *29*, 247−293.
(8) Mahoney, C. M.; Fahey, A. J.; Gillen, G.; Xu, C.; Batteas, J. D. *Appl. Surf. Sci.* **2006**, *252*, 6502−6505.
(9) Nieuwjaer, N.; Poleunis, C.; Delcorte, A.; Bertrand, P. *Surf. Interface Anal.* **2009**, *41*, 6−10.
(10) Möllers, R.; Tuccitto, N.; Torrisi, V.; Niehuis, E.; Licciardello, A. *Appl. Surf. Sci.* **2006**, *252*, 6509−6512.
(11) Sjovall, P.; Rading, D.; Ray, S.; Yang, L.; Shard, A. G. *J. Phys. Chem. B* **2010**, *114*, 769−774.
(12) Miyayama, T.; Sanada, N.; Iida, S.; Hammond, J. S.; Suzuki, M. *Appl. Surf. Sci.* **2008**, *255*, 951−953.
(13) Kozole, J.; Wucher, A.; Winograd, N. *Anal. Chem.* **2008**, *80*, 5293−5301.
(14) Ninomiya, S.; Ichiki, K.; Yamada, H.; Nakata, Y.; Seki, T.; Aoki, T.; Matsuo, J. *Rapid Commun. Mass Spectrom.* **2009**, *23*, 1601−1606.
(15) Lee, J. L. S.; Ninomiya, S.; Matsuo, J.; Gilmore, I. S.; Seah, M. P.; Shard, A. G. *Anal. Chem.* **2010**, *82*, 98−105.
(16) Shard, A. G.; Havelund, R.; Seah, M. P.; Spencer, S. J.; Gilmore, I. S.; Winograd, N.; Mao, D.; Miyayama, T.; Niehuis, E.; Rading, D.; Moellers, R. *Anal. Chem.* **2012**, *84*, 7865−7873.
(17) Tuccitto, N.; Delfanti, I.; Spampinato, V.; Licciardello, A. In *17th International Conference on Secondary Ion Mass Spectrometry*, Toronto, Canada, September 14−18, 2009.
(18) Green, F. M.; Kollmer, F.; Niehuis, E.; Gilmore, I. S.; Seah, M. P. *Rapid Commun. Mass Spectrom.* **2008**, *22*, 2602−2608.
(19) Brison, J.; Muramoto, S.; Castner, D. G. *J. Phys. Chem. C* **2010**, *114*, 5565−5573.
(20) Muramoto, S.; Brison, J.; Castner, D. G. *Surf. Interface Anal.* **2011**, *43*, 58−61.
(21) Cheng, J.; Wucher, A.; Winograd, N. *J. Phys. Chem. B* **2006**, *110*, 8329−8336.
(22) Shard, A. G.; Brewer, P. J.; Green, F. M.; Gilmore, I. S. *Surf. Interface Anal.* **2006**, *39*, 294−298.
(23) Shard, A. G.; Green, F. M.; Brewer, P. J.; Seah, M. P.; Gilmore, I. S. *J. Phys. Chem. B* **2008**, *112*, 2596−2605.
(24) Wucher, A. *Surf. Interface Anal.* **2008**, *40*, 1545−1551.
(25) Czerwinski, B.; Postawa, Z.; Garrison, B. J.; Delcorte, A. *Nucl. Instrum. Methods Phys. Res., Sect. B: Beam Interact. Mater. Atoms* **2012**, DOI: 10.1016/j.nimb.2012.11.030.
(26) Mouhib, T.; Delcorte, A.; Poleunis, C.; Bertrand, P. *Surf. Interface Anal.* **2011**, *43*, 175−178.
(27) Shard, A. G.; Ray, S.; Seah, M. P.; Yang, L. *Surf. Interface Anal.* **2011**, *43*, 1240−1250.